Journal of Bioscience and Bioengineering
VOL. 128 No. 3, 379–383, 2019

www.elsevier.com/locate/jbiosc

# Evaluation of meter-long monolithic columns for selected reaction monitoring mass spectrometry

Yuta Ohtani,[1] Shunsuke Aburaya,[1,2] Hiroyoshi Minakuchi,[3] Natsuko Miura,[1] Wataru Aoki,[1,4,5] and Mitsuyoshi Ueda[1,4,5,*]

*Division of Applied Life Sciences, Graduate School of Agriculture, Kyoto University, Kitashirakawa Oiwake-cho, Sakyo-ku, Kyoto 606-8502, Japan,[1] Japan Society for the Promotion of Science, Kitashirakawa Oiwake-cho, Sakyo-ku, Kyoto 606-8502, Japan,[2] Kyoto Monotech, 1095 Shuzei-cho, Kamigyo-ku, Kyoto 602-8155, Japan,[3] JST, Core Research for Evolutional Science and Technology (CREST), 7 Goban-cho, Chiyoda-ku, Tokyo 102-0076, Japan,[4] and Kyoto Integrated Science & Technology Bio-Analysis Center, 134 Chudoji Minamimachi, Simogyo-ku, Kyoto 600-8813, Japan[5]*

Received 13 December 2018; accepted 8 March 2019
Available online 5 April 2019

**Proteome is extremely complex as many proteins with a large dynamic range are involved. Nano-liquid chromatography/mass spectrometry-based proteomics has made it possible to separate and identify thousands of proteins in one shot. Although the number of identified proteins in proteomics has significantly improved, it is necessary to increase detection sensitivity to clearly identify low-abundant proteins. In this study, we developed meter-long monolithic columns with a small inner diameter and applied them to selected reaction monitoring-based proteomics for improving proteomic detection sensitivity. Bovine serum albumin tryptic digests were analyzed with optimized selected reaction monitoring methods, and separation efficiency and detection sensitivity in each monolithic column were evaluated. As a result, peak capacity increased by about 1.8-fold and peak area of peptide levels increased by about 2.3-fold. Although flow rate was reduced during analysis with columns of a smaller inner diameter, the peak area reproducibility was maintained. These data displayed the value of meter-long monolithic columns with small inner diameter for selected reaction monitoring-based proteomics.**



[**Key words:** Proteomics; Monolithic column; Nano-liquid chromatography; Selected reaction monitoring; Bovine serum albumin]

Proteomics with improved chromatographical and mass spectrometrical techniques enables the identification of thousands of proteins without fractionation (1,2). However, it is still difficult to comprehensively detect all proteins, especially those with low abundance (3). For example, the dynamic range of the human plasma proteome reaches $10^{11}$ (4), and it is difficult to identify low-abundant proteins in non-targeted proteomics because of high noise and ion suppression (5).

To resolve these issues, targeted proteomics by selected reaction monitoring (SRM) is a suitable technique to quantify proteins and peptides with high sensitivity (6,7). This method can quantitate hundreds of peptides in one shot (8,9). In SRM-based proteomics, only pre-selected peptides are analyzed, and other peptides and compounds are excluded by the first quadrupole (Q1) (10,11). Hence, SRM-based proteomics exhibits high signal-to-noise ratio and detection sensitivity. However, further improvement of sensitivity is required for detecting low-abundant proteins with less than 100 copies in a single cell (12,13).

To improve detection sensitivity of these low-abundant proteins, it is important to achieve high separation efficiency and to reduce the chromatography column diameter (14,15). Narrowing the peak width with a high-performance separation medium is necessary for achieving high separation efficiency (16). Unlike conventional particle-packed columns that cause high loading pressure because of a narrow flow path, monolithic columns have small skeletons and large flow paths due to a network structure in which these two components are integrated (17). Low loading pressure can be maintained even if the column is expanded to a meter in length, to achieve high separation efficiency. In a previous study, the number of identified proteins in the *Escherichia coli* proteome increased about 2-fold in non-target proteomics with a 350-cm monolithic column, in comparison with a 15-cm packed column (18). A few studies conducted SRM-based proteomics using monolithic columns (19,20), but meter-long monolithic columns were not used. Although application of meter-long monolithic columns to SRM-based proteomics causes longer analysis time, it is important for realizing highly sensitive analysis with a narrow peak width.

Reducing the inner diameter (ID) of the column is another approach used to improve detection sensitivity (21,22). Separated analytes are ionized by electrospray ionization (ESI) and introduced into a mass spectrometer (MS). In ESI, high voltage is applied to the emitter tip and charged droplets are released into the atmosphere and desolvated. Finally, the analytes become desolvated ions and are detected by MS (23). In this process, the flow rate of liquid chromatography (LC) greatly affects analyte concentration, ionization, and desolvation (24). Reducing the flow rate of LC increases

* Corresponding author at: Division of Applied Life Sciences, Graduate School of Agriculture, Kyoto University, Kitashirakawa Oiwake-cho, Sakyo-ku, Kyoto 606-8502, Japan. Tel./fax: +81 75 753 6112.
*E-mail address:* miueda@kais.kyoto-u.ac.jp (M. Ueda).

1389-1723/$ – see front matter 
https://doi.org/10.1016/j.jbiosc.2019.03.001

the concentration of the eluted analytes, and a decrease in elution volume promotes ionization and desolvation (25). Therefore, reducing the column ID improves MS detection sensitivity. In conventional LC–MS analysis, the peak intensity increased 50-fold by reducing column ID from 2.1 mm to 300 μm (26). There are also studies evaluating the detection sensitivity following reduction of column ID in nano-LC (25).

In this study, we aimed to increase the peak intensity of peptide levels in SRM-based proteomics by reducing the monolithic column ID. It was predicted that a narrow peak width and low column ID would increase the peptide peak area. Our data showed a peak capacity increase by 1.8-fold after lengthening the column (500–1000 mm) and a peak area increase by 2.3-fold by reducing the column ID (100–75 μm). These results indicate that the increase in ionization efficiency caused by reducing the monolithic column ID enhances the sensitivity of SRM-based proteomics.

## MATERIALS AND METHODS

**Reagents** Bovine serum albumin (BSA; product number, P.N. 23209) was purchased from Thermo Fisher Scientific (Waltham, MA, USA). Triethylammonium bicarbonate buffer (TEAB; P.N. T7408) was purchased from Sigma–Aldrich (St. Louis, MO, USA). Acetonitrile (P.N. 018-19853), iodoacetamide (IAA; P.N. 093-02152), and lysyl endopeptidase mass spectrometry grade (Lys-C; P.N. 125-05061) were purchased from Wako Pure Chemical Industries (Osaka, Japan). Methanol (P.N. 21929-23), chloroform (P.N. 08402-13), dithiothreitol (DTT; P.N. 14112-94), deoxycholic acid sodium salt (SDC; P.N. 10726-42), *N*-lauryolsarcosine sodium salt (SLS; P.N. 201-17), ethyl acetate (P.N.; 14746-91), and trifluoroacetic acid (TFA; P.N. 34833-92) were purchased from Nacalai Tesque Inc. (Kyoto, Japan). Ultrapure water (P.N. 11307-76) was purchased from Kanto Chemical Co., Inc (Tokyo, Japan). Sequencing grade modified trypsin (P.N. V5111) was purchased from Promega Corporation (Madison, WI, USA).

**Preparation of analytical samples** Methanol (800 μL), chloroform (200 μL), and water (600 μL) were added to 2.0 mg/mL BSA (200 μL), and the solution was vortexed after each addition. The resultant solution was centrifuged (13,000× *g*, room temperature [RT], 5 min) and separated into two layers. The aqueous (upper) layer was removed, and the organic (lower) layer was vortexed after addition of methanol (600 μL). The resulting solution was centrifuged (13,000× *g*, RT, 5 min). The supernatant was removed, and the precipitate was dried under reduced pressure. Solubilizing buffer (100 μL) comprising 50 mM TEAB, 12 mM SDC, and 12 mM SLS (27) was added to the dried protein pellet. The obtained protein solution was treated with DTT (final concentration, 50 mM) at 37°C for 30 min. After the reaction, IAA (final concentration, 50 mM) was added and incubated at RT for 30 min under light-shielding conditions for carbamidomethylation of cysteine residues. Lys-C (2 μL of 1 μg/μL) was added and incubated at 37°C for 4 h, followed by addition of trypsin (2 μL of 1 μg/μL) and incubation at 37°C overnight. Next, ethyl acetate (100 μL) and trifluoroacetic acid (1 μL) were added to the mixture and vortexed. Thereafter, the mixture was centrifuged (16,000× *g*, RT, 2 min). The organic layer was removed, and the aqueous solution was dried under reduced pressure and dissolved in TEAB solution (100 μL of 50 mM). The resulting peptide solution was desalted using Monospin C18 (GL Science, Tokyo, Japan, P.N. 5010-21701) according to the manufacturer's protocol and eluted with 95% acetonitrile containing 0.1% TFA. The eluate was dried under reduced pressure, dissolved in TEAB (100 μL of 50 mM), and the peptide concentration was determined by BCA assay. Peptides were diluted to 10 fmol/μL (for length evaluation) or 100 fmol/μL (for ID evaluation) and analyzed by LC–MS/MS.

**Nano LC–MS/MS analysis** BSA tryptic digests were analyzed by LC (Ultimate RS3000; Thermo Fisher Scientific) triple quadrupole mass spectrometry (LCMS-8060; Shimadzu, Kyoto, Japan). Monolithic columns (either 500 or 1000 mm) with two different IDs (100 or 75 μm) were prepared according to previous reports (28) and connected directly to a 6-port injection/switching valve (Valco Instruments, Houston, TX, USA). BSA tryptic peptides (10 or 100 fmol/μL) passed 1 μL or 10 nL sample loops and were fully injected into each monolithic column at 1.0 mm/s linear velocity (flow rate, 500 nL/min for 100 μm ID, or 280 nL/min for 75 μm ID). A gradient was produced by changing the mixing ratio of the two eluents: A, 0.1% (v/v) formic acid; and B, acetonitrile containing 0.1% (v/v) formic acid. The gradient commenced with 5% of ratio B with a 20-min hold, was then increased to 40% ratio B for 40 min, and finally increased to 95% ratio B for a 20-min hold, following which the mobile phase was immediately adjusted to its initial composition and held for 20 min to re-equilibrate the column. The autosampler and column oven were maintained at 4°C at 40°C, respectively.

The heat block temperature was set at 200°C and the desolvation line temperature was set at 250°C. BSA tryptic peptides were eluted from the monolithic column and ionized by Fortis Chip (AMR Inc., Tokyo, Japan), followed by MS injection.

**Optimization of SRM methods** All transitions made on Skyline (29) were analyzed using a 100-μm monolithic column. The ionization efficiency at ESI differs depending on the length and sequence of peptides (30), even at the same peptide concentration; therefore, 10 peptides showing high peak area were selected. In addition, four sensitive transitions were selected for one peptide, and these transitions were used as an analytical method (Table S1).

In SRM analysis using a triple quadrupole MS, an analyte is accelerated with collision energy (CE) as it passes through the collision cell (Q2), and fragments are generated by introducing an inert gas (11). Therefore, to optimize CE, 10 CE values in each transition were set and BSA tryptic digests were analyzed. The CE with the highest peak intensity was selected from the obtained results and adopted as the SRM method (Table S1).

## RESULTS

**Comparison of chromatography analyzed by monolithic columns of differing lengths** First, SRM methods for BSA tryptic digests were generated using Skyline (Table S1), and SRM-based analysis was performed on 10-fmol BSA tryptic digests using monolithic columns with an ID of 100 μm and a length of either 500 or 1000 mm (Fig. S1). Peak capacity was about twice as high when using a 1000-mm monolithic column versus that of 500 mm. Peak capacity was calculated using the following Eq. 1. The peak width was calculated by setting the peak start to the point where it stood from the baseline and the peak end to the point where the reduction rate of the intensity reached a constant level. Peak capacity ($P_c$) depends on gradient time ($t_g$) and average of peak width ($W$).

$$P_c = 1 + \frac{t_g}{W} \quad (1)$$

Next, a 1-fmol BSA tryptic digest was analyzed using monolithic columns with two different IDs (i.e., 100 or 75 μm). We first evaluated the retention time, peak half width, and peak capacity. As a result, we found that the retention time became longer by about 1.1-fold as column ID decreased (Table 1). Although we applied the

**TABLE 1.** Comparison of retention times and half widths.

| Peptide sequence | 100 μm | | 75 μm | |
|---|---|---|---|---|
| | RT (min) | Half width (min) | RT (min) | Half width (min) |
| GLVLIAFSQYLQQCPFDEHVK | 68.565 ± 0.084 | 0.150 ± 0.003 | 73.900 ± 0.112 | 0.110 ± 0.006** |
| LVNELTEFAK | 56.864 ± 0.012 | 0.139 ± 0.005 | 62.829 ± 0.125 | 0.106 ± 0.011* |
| SLHTLFGDELCK | 56.561 ± 0.038 | 0.150 ± 0.016 | 62.280 ± 0.119 | 0.119 ± 0.000 |
| LKPDPNTLCDEFK | 53.302 ± 0.051 | 0.229 ± 0.006 | 58.809 ± 0.110 | 0.176 ± 0.022* |
| ECCHGDLLECADDR | 48.934 ± 0.037 | 0.141 ± 0.012 | 54.423 ± 0.169 | 0.084 ± 0.006** |
| DAFLGSFLYEYSR | 67.016 ± 0.099 | 0.150 ± 0.006 | 72.748 ± 0.119 | 0.110 ± 0.006** |
| DDPHACYSTVFDK | 51.430 ± 0.054 | 0.141 ± 0.012 | 56.889 ± 0.126 | 0.097 ± 0.006* |
| LGEYGFQNALIVR | 60.367 ± 0.045 | 0.141 ± 0.006 | 66.384 ± 0.194 | 0.101 ± 0.006** |
| RPCFSALTPDETYVPK | 54.856 ± 0.022 | 0.150 ± 0.006 | 60.429 ± 0.103 | 0.106 ± 0.011** |
| LFTFHADICTLPDTEK | 58.796 ± 0.016 | 0.130 ± 0.006 | 64.576 ± 0.183 | 0.077 ± 0.014** |

Each value represents the mean ± standard deviation of three technical replicates. Underlined C represents carbamidomethylated cysteine. Statistical analysis was performed using *t*-test. Asterisk and double asterisk indicate significant differences ($p < 0.05$ and 0.01, respectively). RT, retention time; half width, peak half width.

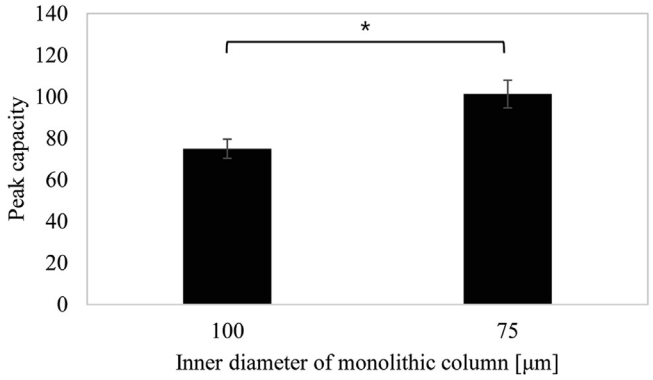


FIG. 1. Comparison of peak capacities. Peak capacities were calculated based on analysis of ten types of peptides derived from BSA tryptic digest. Each value represents the mean ± standard deviation of three technical replicates. Statistical analysis was performed using *t*-test. Asterisk indicates a significant difference ($p < 0.01$) in peak capacities.

same linear velocity in each analysis, diffusion with extra column volume could delay elution times. Half width became small when using the narrow monolithic column, and was almost the same as a previous report (19) (Table 1). Furthermore, peak capacity was improved by using the narrow monolithic column (Fig. 1). This is probably because the diffusion along the column axis ($C_d$) in the Giddings equation shown as Eq. 2 decreased by reducing the column inner diameter, and the peak width improved as the height equivalent to a theoretical plate decreased (31).

$$H = \frac{1}{\left({}^{1}/_{C_e d_P}\right) + \left({}^{D_m}/_{C_m {d_p}^2 u}\right)} + \frac{C_d D_m}{u} + \frac{C_{sm} {d_p}^2 u}{D_m} \qquad (2)$$

The Giddings equation shows that the height equivalent to a theoretical plate ($H$) depends on the linear velocity ($u$), the coefficient accounting for eddy diffusion ($C_e$), the coefficient accounting for molecular diffusion ($C_m$), the coefficient accounting for axial diffusion ($C_d$), the coefficient accounting for the resistance to mass transfer kinetics ($C_{sm}$), particle size ($d_p$), and the diffusion factor ($D_m$).

From these results, reduction of column ID sharpened the peaks. It is considered that reduction of column ID concentrated the analytes.

**TABLE 2.** Peak areas of BSA tryptic peptides analyzed with monolithic columns with different ID.

| Peptide sequence | The ratio of peak area comparing to 100 μm | |
|---|---|---|
| | 100 μm | 75 μm |
| GLVLIAFSQYLQQCPFDEHVK | 1.00 ± 0.22 | 5.35 ± 0.18** |
| LVNELTEFAK | 1.00 ± 0.02 | 1.59 ± 0.16** |
| SLHTLFGDELCK | 1.00 ± 0.05 | 2.01 ± 0.13** |
| LKPDPNTLCDEFK | 1.00 ± 0.04 | 2.49 ± 0.06** |
| ECCHGDLLECADDR | 1.00 ± 0.11 | 2.12 ± 0.38* |
| DAFLGSFLYEYSR | 1.00 ± 0.07 | 1.86 ± 0.09** |
| DDPHACYSTVFDK | 1.00 ± 0.11 | 1.47 ± 0.10* |
| LGEYGFQNALIVR | 1.00 ± 0.07 | 2.74 ± 0.65* |
| RPCFSALTPDETYVPK | 1.00 ± 0.05 | 2.70 ± 0.07** |
| LFTFHADICTLPDTEK | 1.00 ± 0.05 | 2.12 ± 0.61 |
| Geometric mean | 1 | 2.28 |

Each value represents mean ± standard deviation of three technical replicates. Underlined C represents carbamidomethylated cysteine. Statistical analysis was performed using *t*-test. Asterisk and double asterisk indicate significant differences ($p < 0.05$ and 0.01, respectively).

**TABLE 3.** Signal-to-noise ratio of BSA tryptic peptides analyzed with monolithic columns with different ID.

| Peptide sequence | The ratio of S/N ratio comparing to 100 μm | |
|---|---|---|
| | 100 μm | 75 μm |
| GLVLIAFSQYLQQCPFDEHVK | 1.00 ± 0.23 | 8.75 ± 1.00** |
| LVNELTEFAK | 1.00 ± 0.02 | 5.99 ± 0.45** |
| SLHTLFGDELCK | 1.00 ± 0.09 | 2.71 ± 0.25** |
| LKPDPNTLCDEFK | 1.00 ± 0.06 | 27.45 ± 2.11** |
| ECCHGDLLECADDR | 1.00 ± 0.08 | 1.65 ± 0.32* |
| DAFLGSFLYEYSR | 1.00 ± 0.05 | 2.10 ± 0.08** |
| DDPHACYSTVFDK | 1.00 ± 0.17 | 3.21 ± 0.30** |
| LGEYGFQNALIVR | 1.00 ± 0.09 | 3.51 ± 0.86* |
| RPCFSALTPDETYVPK | 1.00 ± 0.08 | 2.71 ± 0.16** |
| LFTFHADICTLPDTEK | 1.00 ± 0.04 | 9.75 ± 2.90* |

Each value represents mean ± standard deviation of three technical replicates. Underlined C represents carbamidomethylated cysteine. Statistical analysis was performed using *t*-test. Asterisk and double asterisk indicate significant differences ($p < 0.05$ and 0.01, respectively).

**Evaluation of peak areas for each peptide** BSA tryptic digests were analyzed using monolithic columns (IDs of 100 or 75 μm), and the noise levels between the analyses using the 100 and 75 μm columns were nearly equal. The peak areas of each peptide were evaluated (Table 2). Among the 10 peptides, when the column with 75-μm ID was used, the peak areas of nine peptides were significantly increased and the geometric mean of increase rate of detection sensitivity was 2.28-fold. In addition, the signal-to-ratio of the 10 peptides was improved by reducing column ID (Table 3). This is because the peaks became sharp and the peak intensity was improved by reducing column ID. Comparing the limit of detection of the two most sensitive peptides, monolithic columns with small ID enabled to detect smaller amount of peptides (Table 4). Here, concentrations whose signal-to-noise ratios were over three were defined as the limit of detection. From these results, it was confirmed that the peak intensity increased by using SRM-based proteomics using a long monolithic column with small diameter.

Subsequently, the reproducibility of the peak areas was evaluated. As a result, even with ID reduction, the median coefficient of variation (CV) value did not change (Fig. 2), suggesting the maintenance of reproducibility even in analyses using monolithic columns of reduced ID.

## DISCUSSION

Previous studies showed that meter-long monolithic columns were effective for analyzing complex proteomes, such as the symbiotic or infectious disease proteome in shotgun proteomics (32,33). This is because peaks became sharper due to a longer column length, consistent with the following Eq. 3 (34):

$$R = \frac{1}{4}\sqrt{N}\left(\frac{\alpha - 1}{\alpha}\right)\left(\frac{k}{1 + k}\right) \qquad (3)$$

The resolution ($R$) depends on the number of theoretical plates ($N$), the separation factor ($\alpha$), and retention factor ($k$). Because the

**TABLE 4.** Limit of detection of BSA tryptic peptides analyzed with monolithic columns with different ID.

| Peptide sequence | Limit of detection | |
|---|---|---|
| | 100 μm | 75 μm |
| DAFLGSFLYEYSR | 30 atmol | 10 atmol |
| RPCFSALTPDETYVPK | 80 atmol | 20 atmol |

Underlined C represents carbamidomethylated cysteine. Concentrations whose signal-to-noise ratios were over three were defined as the limit of detection.

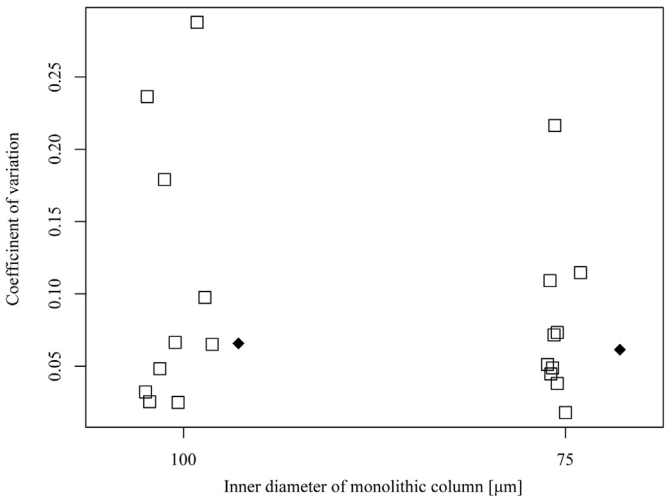


FIG. 2. Comparison of coefficient of variation of peak areas. Values of coefficient of variation (CV) were calculated based on analysis of ten types of peptides derived from BSA tryptic digest. The unfilled point represents the CV value of each peptide. Black point represents the median at each ID.

number of theoretical plates increases in proportion to the length of the column, it is considered that separation efficiency increases by using a longer column.

More sensitive analysis is required to analyze low-abundant proteins. In this study, we showed that combining SRM-based proteomics and meter-long monolithic columns improved sensitivity. Lengthening monolithic columns from 500 to 1000 mm increased the peak capacity by 1.8 fold. Furthermore, reducing the ID from 100 to 75 μm increased the peak area of BSA tryptic digests by about 2.28-fold on average. Theoretically, the reduction of I.D. from 100 μm to 75 μm was predicted to increase sensitivity by 1.8-fold. This difference might be derived from the promotion of desolvation with a low flow rate, in addition to analyte concentration. Recently Hara et al. developed a silica monolithic column with an ID of 5 μm (35), which is expected to further improve detection sensitivity.

In conclusion, this study showed that detection sensitivity is increased by reducing the ID of monolithic columns in SRM-based proteomics. This method could prove to be useful for the effective detection of trace amounts of proteins.

Supplementary data to this article can be found online at https://doi.org/10.1016/j.jbiosc.2019.03.001.

## ACKNOWLEDGMENTS

This work was supported by JST CREST (Grant Number JPMJCR16G2), Japan.

## References

1. **Mann, M., Kulak, N. A., Nagaraj, N., and Cox, J.:** The coming age of complete, accurate, and ubiquitous proteomes, Mol. Cell, **49**, 583–590 (2013).
2. **Ong, S. E. and Mann, M.:** Mass spectrometry-based proteomics turns quantitative, Nat. Chem. Biol., **1**, 252–262 (2005).
3. **Liebermeister, W., Noor, E., Flamholz, A., Davidi, D., Bernhardt, J., and Milo, R.:** Visual account of protein investment in cellular functions, Proc. Natl. Acad. Sci. USA, **111**, 8488–8493 (2014).
4. **Omenn, G. S., States, D. J., Adamski, M., Blackwell, T. W., Menon, R., Hermjakob, H., Apweiler, R., Haab, B. B., Simpson, R. J., Eddes, J. S., and other 30 authors:** Overview of the HUPO Plasma Proteome Project: results from the pilot phase with 35 collaborating laboratories and multiple analytical groups, generating a core dataset of 3020 proteins and a publicly-available database, Proteomics, **5**, 3226–3245 (2005).
5. **Bantscheff, M., Schirle, M., Sweetman, G., Rick, J., and Kuster, B.:** Quantitative mass spectrometry in proteomics: a critical review, Anal. Bioanal. Chem., **389**, 1017–1031 (2007).
6. **Picotti, P., Bodenmiller, B., Mueller, L. N., Domon, B., and Aebersold, R.:** Full dynamic range proteome analysis of *S. cerevisiae* by targeted proteomics, Cell, **138**, 795–806 (2009).
7. **Anderson, L. and Hunter, C. L.:** Quantitative mass spectrometric multiple reaction monitoring assays for major plasma proteins, Mol. Cell. Proteomics, **5**, 573–588 (2006).
8. **Vidova, V. and Spacil, Z.:** A review on mass spectrometry-based quantitative proteomics: targeted and data independent acquisition, Anal. Chim. Acta, **964**, 7–23 (2017).
9. **Kusebauch, U., Campbell, D. S., Deutsch, E. W., Chu, C. S., Spicer, D. A., Brusniak, M. Y., Slagel, J., Sun, Z., Stevens, J., Grimes, B., and other 17 authors:** Human SRMAtlas: a resource of targeted assays to quantify the complete human proteome, Cell, **166**, 766–778 (2016).
10. **Surinova, S., Huttenhain, R., Chang, C. Y., Espona, L., Vitek, O., and Aebersold, R.:** Automated selected reaction monitoring data analysis workflow for large-scale targeted proteomic studies, Nat. Protocols, **8**, 1602–1619 (2013).
11. **Picotti, P. and Aebersold, R.:** Selected reaction monitoring-based proteomics: workflows, potential, pitfalls and future directions, Nat. Methods, **9**, 555–566 (2012).
12. **Ghaemmaghami, S., Huh, W., Bower, K., Howson, R. W., Belle, A., Dephoure, N., O'Shea, E. K., and Weissman, J. S.:** Global analysis of protein expression in yeast, Nature, **425**, 737–741 (2003).
13. **Kulak, N. A., Pichler, G., Paron, I., Nagaraj, N., and Mann, M.:** Minimal, encapsulated proteomic-sample processing applied to copy-number estimation in eukaryotic cells, Nat. Methods, **11**, 319–324 (2014).
14. **Churchwell, M. I., Twaddle, N. C., Meeker, L. R., and Doerge, D. R.:** Improving LC-MS sensitivity through increases in chromatographic performance: comparisons of UPLC-ES/MS/MS to HPLC-ES/MS/MS, J. Chromatogr. B, **825**, 134–143 (2005).
15. **Hopfgartner, G., Bean, K., Henion, J., and Henry, R.:** Ion-spray mass-spectrometric detection for liquid-chromatography: a concentration- or a mass-flow-sensitive device? J. Chromatogr. A, **647**, 51–61 (1993).
16. **Specht, H. and Slavov, N.:** Transformative opportunities for single-cell proteomics, J. Proteome Res., **17**, 2565–2571 (2018).
17. **Wilson, S. R., Vehus, T., Berg, H. S., and Lundanes, E.:** Nano-LC in proteomics: recent advances and approaches, Bioanalysis, **7**, 1799–1815 (2015).
18. **Iwasaki, M., Miwa, S., Ikegami, T., Tomita, M., Tanaka, N., and Ishihama, Y.:** One-dimensional capillary liquid chromatographic separation coupled with tandem mass spectrometry unveils the *Escherichia coli* proteome on a microarray scale, Anal. Chem., **82**, 2616–2620 (2010).
19. **Vehus, T., Seterdal, K. E., Krauss, S., Lundanes, E., and Wilson, S. R.:** Comparison of commercial nanoliquid chromatography columns for fast, targeted mass spectrometry-based proteomics, Futur. Sci. Oa, **2**, FSO119 (2016).
20. **Borges, V., Yang, E., Dunn, J., and Henion, J.:** High-throughput liquid chromatography-tandem mass spectrometry determination of bupropion and its metabolites in human, mouse and rat plasma using a monolithic column, J. Chromatogr. B, **804**, 277–287 (2004).
21. **Needham, S. R. and Valaskovic, G. A.:** Microspray and microflow LC-MS/MS: the perfect fit for bioanalysis, Bioanalysis, **7**, 1061–1064 (2015).
22. **Saito, Y., Jinno, K., and Greibrokk, T.:** Capillary columns in liquid chromatography: between conventional columns and microchips, J. Sep. Sci., **27**, 1379–1390 (2004).
23. **Fenn, J. B., Mann, M., Meng, C. K., Wong, S. F., and Whitehouse, C. M.:** Electrospray ionization for mass-spectrometry of large biomolecules, Science, **246**, 64–71 (1989).
24. **Gale, D. C. and Smith, R. D.:** Small-volume and low flow-rate electrospray-ionization mass-spectrometry of aqueous samples, Rapid Commun. Mass Spectrom., **7**, 1017–1021 (1993).
25. **Zhu, Y., Zhao, R., Piehowski, P. D., Moore, R. J., Lim, S., Orphan, V. J., Pasa-Tolic, L., Qian, W. J., Smith, R. D., and Kelly, R. T.:** Subnanogram proteomics: impact of LC column selection, MS instrumentation and data analysis strategy on proteome coverage for trace samples, Int. J. Mass Spectrom., **427**, 4–10 (2018).
26. **Buckenmaier, S., Miller, C. A., van de Goor, T., and Dittmann, M. M.:** Instrument contributions to resolution and sensitivity in ultra high performance liquid chromatography using small bore columns: comparison of diode array and triple quadrupole mass spectrometry detection, J. Chromatogr. A, **1377**, 64–74 (2015).
27. **Masuda, T., Tomita, M., and Ishihama, Y.:** Phase transfer surfactant-aided trypsin digestion for membrane proteome analysis, J. Proteome Res., **7**, 731–740 (2008).
28. **Ishizuka, N., Minakuchi, H., Nakanishi, K., Soga, N., Nagayama, H., Hosoya, K., and Tanaka, N.:** Performance of a monolithic silica column in a capillary under pressure-driven and electrodriven conditions, Anal. Chem., **72**, 1275–1280 (2000).
29. **Bereman, M. S., MacLean, B., Tomazela, D. M., Liebler, D. C., and MacCoss, M. J.:** The development of selected reaction monitoring methods for targeted proteomics via empirical refinement, Proteomics, **12**, 1134–1141 (2012).

30. **Uchida, Y., Tachikawa, M., Obuchi, W., Hoshi, Y., Tomioka, Y., Ohtsuki, S., and Terasaki, T.:** A study protocol for quantitative targeted absolute proteomics (QTAP) by LC-MS/MS: application for inter-strain differences in protein expression levels of transporters, receptors, claudin-5, and marker proteins at the blood-brain barrier in ddY, FVB, and C57BL/6J mice, Fluids Barriers CNS, **10**, 21 (2013).
31. **Bruns, S., Grinias, J. P., Blue, L. E., Jorgenson, J. W., and Tallarek, U.:** Morphology and separation efficiency of low-aspect-ratio capillary ultrahigh pressure liquid chromatography columns, Anal. Chem., **84**, 4496−4503 (2012).
32. **Tatsukami, Y., Nambu, M., Morisaka, H., Kuroda, K., and Ueda, M.:** Disclosure of the differences of *Mesorhizobium loti* under the free-living and symbiotic conditions by comparative proteome analysis without bacteroid isolation, BMC Microbiol., **13**, 180 (2013).
33. **Kitahara, N., Morisaka, H., Aoki, W., Takeda, Y., Shibasaki, S., Kuroda, K., and Ueda, M.:** Description of the interaction between *Candida albicans* and macrophages by mixed and quantitative proteome analysis without isolation, AMB Express, **5**, 127 (2015).
34. **Snyder, L. R. and Kirkland, J. J.:** Basic concepts and control of separation, pp. 15−82, in: Snyder, L. R. and Kirkland, J. J. (Eds.), Introduction to modern liquid chromatography, 2nd ed. John Wiley & Sons, Hoboken (1979).
35. **Hara, T., Futagami, S., De Malsche, W., Eeltink, S., Terryn, H., Baron, G. V., and Desmet, G.:** Chromatographic properties of minimal aspect ratio monolithic silica columns, Anal. Chem., **89**, 10948−10956 (2017).